ACS Catalysis

Research Article

pubs.acs.org/acscatalysis

Versatile and Efficient Immobilization of 2-Deoxyribose-5-phosphate Aldolase (DERA) on Multiwalled Carbon Nanotubes

Fabiana Subrizi,[†,∥] Marcello Crucianelli,*[,†] Valentina Grossi,[†] Maurizio Passacantando,[†] Giorgia Botta,[‡] Riccarda Antiochia,[§] and Raffaele Saladino*[,‡]

[†]Department of Physical and Chemical Sciences, University of L'Aquila, Via Vetoio, I-67100 Coppito (AQ), Italy

[‡]Department of Ecology and Biology, University of Tuscia, Largo dell'Università, 01100 Viterbo (VT), Italy

[§]Department of Chemistry and Drug Technologies, Sapienza University of Rome, Piazzale Aldo Moro 5, 00185 Rome (RM), Italy

Supporting Information

ABSTRACT: A series of five new catalysts **I**–**V** based upon the immobilization of 2-deoxyribose-5-phosphate aldolase (DERA) on multiwalled carbon nanotubes (MWCNTs) were prepared, and their use for the formation of the C–C bond via cross-aldol condensation, under environmental friendly conditions, was studied. Among the various employed procedures, the direct immobilization of the enzyme through ionic exchange interactions on oxidized multiwalled carbon nanotubes (ox-MWCNTs) afforded the most efficient catalyst **I**. This catalyst was shown to be stable with a high tolerance to acetaldehyde, and it maintained its activity for several days, being reused for five runs. The versatility of catalyst **I** in cross-aldol condensation was evaluated in the reaction of acetaldehyde alone (self-condensation) or in the presence of chloro-acetaldehyde. The corresponding cyclic lactols were obtained in higher yield than native DERA.

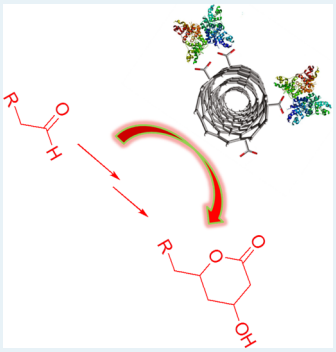

KEYWORDS: *aldolase, DERA, carbon nanotubes, aldol condensation, biocatalyst, supported enzyme*

INTRODUCTION

The asymmetric aldol condensation is one of the most powerful reactions in organic chemistry, during which two carbonyl compounds are combined to form β-hydroxy carbonyl derivatives (C–C bond formation).[1] The enzyme 2-deoxy-ribose-5-phosphate aldolase (DERA), a type I aldolase, catalyzes the aldol condensation of prochiral aldehydes with excellent stereoselectivity and high yield.[2]

DERA is unique among aldolases, being able to catalyze the condensation between two or more aldehydes in a sequential manner and with low substrate specificity.[3,4] This greatly simplifies the preparation of synthons and natural compounds,[5] representing an attractive alternative for green and sustainable manufactures.[6] For example, the aldol condensation catalyzed by DERA between three molecules of acetaldehyde affords 2,4,6-trideoxyhexoses,[4a] that are valuable intermediates for the production of atorvastatin[7] and other cholesterol-lowering drugs.[8]

DERA has been successfully overexpressed in *E. coli*, and large quantities of the enzyme can be simply and readily obtained: the protein consists of 259 amino acids, with a molecular weight of 27.7 kDa. The purified enzyme may exist as both a monomer and dimer,[3d] and analysis of DERA from the *Streptococcus mutans* strain GS-5 showed a p*I* (isoelectric point) of 5.44.[3a]

Nevertheless, the use of DERA for large scale productions remains an open challenge. Some of the major drawbacks arise from the possibility of substrate inhibition and the long reaction times usually associated with low stability. In the case of DERA from *E. coli*, the dissociation of the subunits (in the dimeric form) can produce the loss of activity. This problem may be overcome by the use of proper experimental conditions, including protein engineering, physical or chemical cross-linking, and immobilization on appropriate supports.[9b]

In some cases, limitations have mainly been addressed by discovering genetically improved DERAs or developing fed-batch processes,[9] while only few examples of immobilization of DERA on solid supports have been reported.[10] Immobilization can improve the activity and stability of the enzyme, allowing a better handling and expanding its use under unconventional operative conditions.[11] The main advantages derive from the easy product isolation, the high enzyme loading, and the possibility of reuse of the catalyst several times, thus minimizing the cost of the processes.[12]

Multiwalled carbon nanotubes (MWCNTs) are excellent supports for enzyme immobilization, because they offer a high surface area for loading, as well as biocompatibility and mechanical resistance.[13] They consist of several layers of graphitic sheets, rolled up into a cylindrical shape surrounding a central tube, with lengths in the micrometers and diameters up to 100 nm.[14]

Received: April 18, 2014
Revised: July 22, 2014
Published: July 30, 2014

Here we describe the immobilization of DERA from *E. coli* on MWCNTs. Five novel catalysts (**I**–**V**) have been prepared based on the immobilization of DERA on both pristine and oxidized MWCNTs, with or without the use of polyelectrolytes or aromatic acid to increase the stability of the system. After structural characterization, the most active catalyst **I** was used in selected cross-aldol condensation of acetaldehyde and chloroacetaldehyde to afford the corresponding lactol derivatives in satisfying yield (81 and 89% yield, respectively).

RESULTS AND DISCUSSION

Preparation of the Support and Optimization of the Immobilization Procedures. Covalent and noncovalent conjugation methods have been reported for the immobilization of enzymes, each with its own associated advantages and disadvantages.[15] Noncovalent attachment preserves the unique properties of both enzymes and support, but the immobilized protein can be gradually lost during the use of the catalyst. On the other hand, the covalent attachment improves stability and reduces leaching, but it could severely damage the structural integrity of the enzyme. The comparison between different techniques can provide guidelines for the selection of immobilization conditions that are optimal to maintain the enzyme activity as closely as possible to its native state.[15] With this aim, we explored a panel of noncovalent procedures for physical adsorption of DERA onto pristine or oxidized MWCNTs (as for catalysts **I**, **III**, and **IV**), or in a more specific way, by the assistance of polyelectrolytes (catalyst **II**) or through a tethering agent (catalyst **V**). In the first selected approach, the MWCNTs were oxidized by prolonged sonication at 25 °C in a mixture of concentrated nitric and sulfuric acids (v/v, 1:3) for 4 h, followed by extensive washing in deionized water until the filtrate was neutral. The acidic treatment allowed the removal of impurities (residual contamination and amorphous carbons) and the introduction of carboxyl and hydroxyl groups at the ends or sidewall defects of the structure, which increase their dispersion in aqueous solutions. The solubility in water, as a measure of the extent of the oxidation, was verified by UV–vis spectroscopy (maximum absorbance at 500 nm).[16] A linear relationship between absorbance and concentration of oxidized nanotubes (ox-MWCNTs) was observed, with the solution being stable for more than 1 week. For the preparation of catalyst **I** (Figure 1), the ox-MWCNTs were treated with a solution of DERA for 40 min at 25 °C followed by centrifugation to remove the enzyme that was not immobilized.

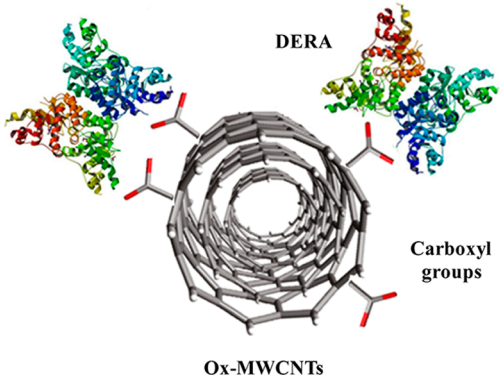

Figure 1. Schematic representation of catalyst **I**.

In particular, ox-MWCNTs were treated with different amounts of DERA (with the ratio of ox-MWCNTs:DERA ranging from 10 to 45 mg/mg, respectively; Table 1, entries 2–5) in sodium acetate buffer (0.1 M, pH 5.5) at 25 °C, and the effectiveness of the immobilization was evaluated by analyzing the residual activity in the waste waters. The activity of native DERA and catalyst **I** was measured under standard conditions,[5b] following the oxidation of NADH in the conversion of glyceraldehyde 3-phosphate (G-3-P) [one of the 2-deoxy-D-ribose-5-phosphate (DRP) cleavage products] to glycerol 3-phosphate by the use of triose-phosphate isomerase (TPI) and glycerol-3-phosphate dehydrogenase (GDH) (Scheme 1).

Table 1. Activity and Immobilization Yields for Catalysts I–V

Entry	Catalyst[a]	Support/DERA ratio (mg/mg)	Immobilization Yield[b] (%)	Activity Yield[b] (%)	Activity[b] (U/mg)
1	DERA				1.51[c]
2	**I**	10	65	1.0	0.13
3	**I**	20	89	2.5	0.56
4	**I**	35	>98	18.0	1.00
5	**I**	45	>98	4.2	0.60
6	**II**	10[d]	10	34.0	0.05
7	**II**	20[d]	19	41.0	0.08
8	**II**	35[d]	27	54.0	0.11
9	**II**	35[e]	32	55.0	0.16
10	**II**	35[f]	35	56.0	0.20
11	**II**	35[e,g]	33	55.0	0.18
12	**III**	35	>98	3.0	0.02
13	**IV**	10	85	4.0	0.04
14	**IV**	20	91	6.0	0.07
15	**IV**	35	98	8.0	0.09
16	**IV**	45	94	14.0	0.04
17	**V**	10	88	11.0	0.15
18	**V**	20	92	55.0	0.16
19	**V**	35	>98	15.0	0.15

[a]Catalytic systems: **I** = ox-MWCNTs/DERA; **II** = ox-MWCNTs/PDDA/DERA; **III** = ox-MWCNTs/DERA/PDDA; **IV** = MWCNTs/DERA; **V** = MWCNTs/PBA/DERA. [b]Average errors were ca. 0.1% for immobilization yield and 0.1–0.2% for both activity yield and activity. [c]This value is in accordance with ref 10c. [d]Values obtained for a loading time of 40 min. [e]Value obtained for a loading time of 4 h. [f]Value obtained for a loading time of 6 h. [g]Value obtained using PHA instead of PDDA.

The activity (defined as the amount of DERA required to catalyze the cleavage of 1 μmol of DRP *per* minute in Tris-HCl buffer at pH 7.5) was expressed as activity units (U) per milligram of support (eq 1), where U_x is the activity (units) of the immobilized enzyme and $W_{support}$ is the weight (mg) of ox-MWCNTs.

$$\text{Activity (U/mg)} = U_x/W_{support} \quad (1)$$

The activity and immobilization yields were also evaluated (eqs 2 and 3, respectively):

$$\text{Activity Yield (\%)} = [U_x/(U_a - U_r)] \times 100 \quad (2)$$

$$\text{Immobilization Yield (\%)} = [(U_a - U_r)/U_a] \times 100 \quad (3)$$

where U_a is the total activity of the enzyme added in the solution and U_r is the residual activity in washing solutions. As

dx.doi.org/10.1021/cs500511c | ACS Catal. 2014, 4, 3059–3068

Scheme 1. Enzymatic Assay of DERA[a]

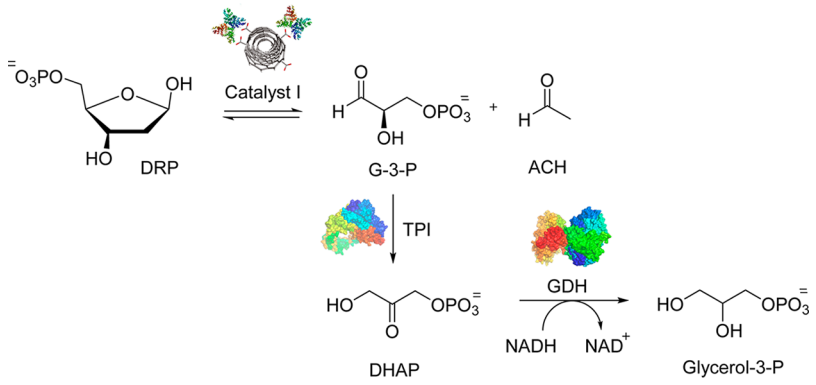

[a]Abbreviations used: DRP (2-deoxyribose-5-phosphate), ACH (acetaldehyde), G-3-P (glyceraldehyde-3-phosphate), TPI (triose-phosphate isomerase), DHAP (dihydroxyacetone phosphate), GDH (glycerol-3-phosphate dehydrogenase), NADH (ß-nicotinamide adenine dinucleotide, reduced form), NAD+ (ß-nicotinamide adenine dinucleotide, oxidized form).

reported in Table 1 (entries 2–5), the activity increased by increasing the value of the support/DERA ratio (dilution parameter), with the maximum (1.0 U) at the value of 35 (Table 1, entry 4). The immobilization and activity yields showed a similar behavior, confirming the positive role of the dilution parameter to reduce possible negative "close packing" effects.[17] On the other hand, the low value (18%) of the activity yield (Table 1, entry 4) implies that only a small fraction of the immobilized enzyme is active. Further dilution of the system (e.g., support/DERA ratio = 45; Table 1, entry 5) did not increase the activity or the activity yield of the catalyst, thus representing a critical end-point. A similar trend has been previously reported for DERA[5b] and for other enzymes immobilized on MWCNTs.[17a] It must be pointed out that the activity of catalyst **I** is higher than that of native DERA when similar amounts of free or supported enzyme are compared (Table 1, entry 4 vs entry 1).

Depending on the pH of the solution and the isoelectric point, the surface of the enzyme may bear charges.[12,18] Based on this assumption, the immobilization of DERA was also performed by applying the layer by layer (LbL) technique, consisting in the deposition of charged polyelectrolytes on the support[19] which usually can stabilize the enzyme.[20] ox-MWCNTs were treated with positively charged poly(diallyl dimethylammonium chloride) (PDDA) in NaCl solution (0.5 M) under orbital shaking,[21] to yield ox-MWCNTs/PDDA. The residual PDDA in the solution was evaluated by UV–vis analysis of supernatant in the presence of Comassie Brillant Blue (CBB).[22] Catalyst **II** (that is, ox-MWCNTs/PDDA/DERA; Figure 2) was then prepared by addition of DERA in sodium acetate buffer (0.1 M, pH 5.5) for 40 min at 25 °C, under the experimental conditions previously reported for catalyst **I** (Table 1, entries 6–8). Attempts to carry out the immobilization at pH 7.0 (0.1 M, sodium phosphate buffer) lead to low active catalyst.

Catalyst **II** showed an immobilization yield lower than that for **I** even at the highest value of the support/DERA ratio (Table 1, entry 8 vs entry 4). As a consequence, a low value of activity (0.11 U) was observed. With respect to activity yield, ca. 50% of DERA maintained its catalytic activity after the immobilization (Table 1, entry 8), suggesting a beneficial effect of PDDA on the stability of the enzyme. This value is greater than that previously obtained for catalyst **I**, in which case only ca. 20% of initial activity was maintained (Table 1, entry 4). On

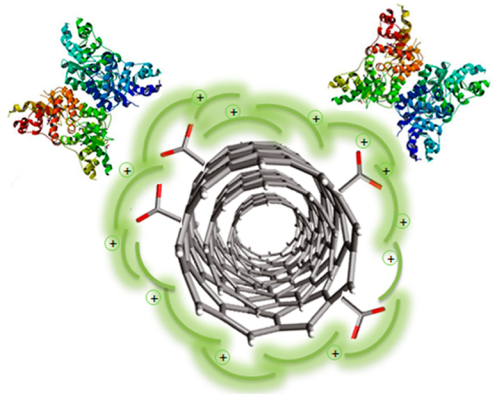

Figure 2. Schematic representation of catalyst **II**: PDDA (green).

the basis of these data, further experiments have been performed to improve the immobilization yield (and possibly the activity) of catalyst **II**, increasing the loading times (4 and 6 h, respectively; Table 1, entries 9 and 10) and, in a selected case, replacing PDDA with polyallylamine hydrochloride (PHA; Table 1, entry 11). Under these experimental conditions, a gradual improvement of the immobilization yield was observed, but the activity of catalyst **II** was still significantly lower than that of **I**, probably due to the low amount of enzyme immobilized on the support. Note that the reversed process, that is the coating of catalyst **I** with PDDA (at the optimal value of the support/DERA ratio), yielded the very low active catalyst **III** (ox-MWCNTs/DERA/PDDA, Figure 3) (Table 1, entry 12). Diffusional phenomena in the polyelectrolyte layer, able to modify the DERA accessibility and reactivity, may be responsible for these findings.

At this stage, the use of pristine MWCNTs was evaluated by exploring the role of hydrophobic and van der Waals interactions, in accordance with data previously reported for lipase and other enzymes.[23] MWCNTs were suspended in sodium acetate buffer (pH 5.5) and subjected to prolonged sonication to increase the surface available for enzyme immobilization. A DERA solution in the same buffer was then added (different support/DERA ratio ranging from 10 to 45 mg/mg, Table 1 entries 13–16) and the mixture shaken for 40 min at 25 °C to yield catalyst **IV** (MWCNTs/DERA; Figure 4). In this case, the low values of both activity and activity yield (0.09 U and 8.0%, respectively), in spite of the relatively high

dx.doi.org/10.1021/cs500511c | ACS Catal. 2014, 4, 3059–3068

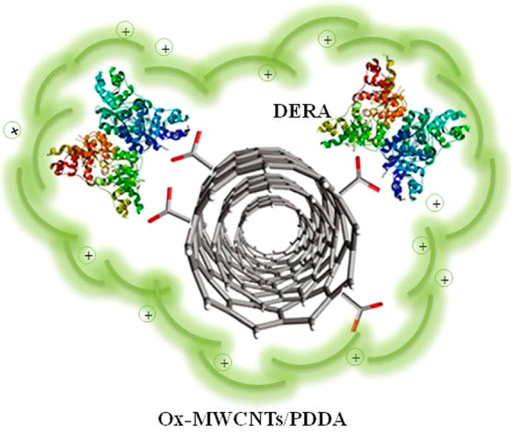

Figure 3. Schematic representation of catalyst **III**: PDDA (green).

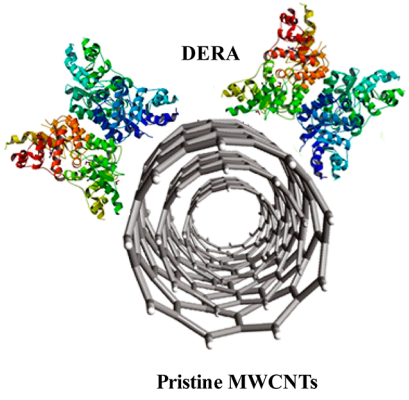

Figure 4. Schematic representation of catalyst **IV**.

efficiency of enzyme immobilization (see, for example, Table 1, entry 15), suggest an extensive process of deactivation of DERA as a result of immobilization. Proteins can undergo conformational changes when immobilized, depending on the nature of the support. In the case of MWCNTs, large lipophilic areas are required for van der Waals interactions. Since the surface of the enzyme that is exposed to water is characterized by hydrophilic residues,[24] conformational changes are necessary to exhibit the hydrophobic area toward the support. This process can alter the enzyme activity, causing denaturation upon adsorption. Thus, DERA can behave differently depending on the properties of the support, which can affect its conformation in a fundamentally different manner.[25]

Finally, a supramolecular approach based on ionic exchange interactions between DERA and pyrenebutyric acid (PBA, pK_a = 4.8), which acts as a tethering agent on the surface of MWCNTs, was used.[26] As schematically shown in Figure 5, PBA was adsorbed by means of a $\pi-\pi$ stacking on the surface of a pristine nanotube.

Briefly, MWCNTs were dispersed in EtOH containing PBA at 25 °C by combination of sonication (2 h) and shaking (150 rpm, overnight). The MWCNTs/PBA system was treated with different support/DERA ratios (ranging from 10 to 35 mg/mg, Table 1 entries 17−19) in 0.1 M sodium acetate buffer, at 25 °C. Catalyst **V** was easily recovered by centrifugation. Compared with catalyst **IV**, the use of PBA led to a slightly more active catalyst (Table 1, entries 13−15 vs entries 17−19) although still far away from the performance of catalyst **I**, which was definitively identified as the most active one. On the basis

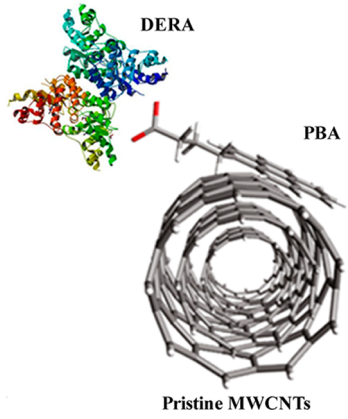

Figure 5. Schematic representation of catalyst **V**.

of data reported in the literature, catalyst **I** showed a better, or comparable, reactivity with respect to previously reported systems based on the covalent immobilization of DERA (from *E. coli*) on *p*-benzoquinone/amino acids support[10c] or mesocellular siliceous foam (MCF),[10a] respectively, or by immobilization of genetically modified DERA (from *Klebsiella pneumonia*) on interparticle pore type mesoporous silica (IMS).[10b]

Scanning Electron Microscopy (SEM) and Atomic Force Microscopy (AFM). The catalysts **I**−**II** and **IV**−**V** were analyzed by both scanning electron microscopy (SEM) and atomic force microscopy (AFM) to verify the morphology and size of MWCNTs in the overall steps of the preparation procedure. Figure 6 shows SEM images and corresponding AFM images[27] of selected areas of different samples. Individual MWCNTs were found. The corresponding AFM images (Figure 6b, d, f, and h) show the detail of a single nanotube immobilized on Si; the white areas, which are higher than the substrate, are dragged from the AFM tip during the scanning. Similar AFM images of pristine and functionalized MWCNTs have been previously obtained.[17a]

In Figure 6a and b, two short nanotubes of catalyst **I** (Table 1, entry 4) are shown. The lighter rectangular areas were produced by the SEM electronic beam during image acquisition, and we can see clearly how the beam changes the surface morphology of the substrate. Fragments of catalyst **II** (Table 1, entry 8) are reported in Figure 6c and d. In this case it was more difficult to disperse and identify the functionalized nanotubes, and those identified appear very tangled. The white area is a part of nanotube dragged from the AFM tip during the scanning.

Catalyst **IV** (Table 1, entry 13) is shown in Figure 6e and f. Nanotubes were easily dispersed and appear not broken. The upper end of the nanotube was pulled away by the AFM tip during scanning, forming a tangle higher than the structure of the nanotube. Catalyst **V** (Table 1, entry 19) is reported in Figure 6g and h. In this case the dispersion in milli-Q water did not break the nanotubes that appear long and well-defined.

Figure 7 reports the high-resolution AFM images (bidimensional part a and tridimensional part b) of the same catalysts (**I**−**II** and **IV**−**V**) and the related image profiles (part c) for selected directions (line in bidimensional AFM images, part a). The surface of catalyst **I** appears to be enveloped by a nonuniform coating (Figure 7a); the maximal height (h) and width at half-height (d), evaluated by a profile analysis (Figure 7c), for the most uniform structure were 69.5 ± 0.5 and 160 ±

dx.doi.org/10.1021/cs500511c | ACS Catal. 2014, 4, 3059−3068

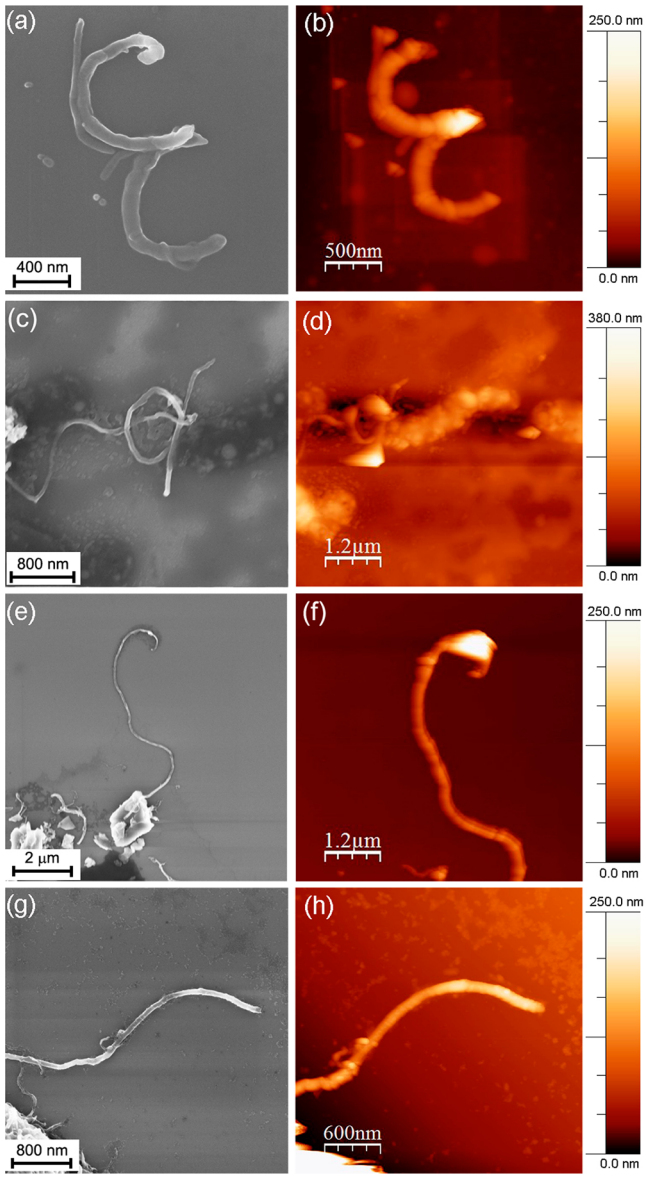

Figure 6. SEM and AFM images of catalysts **I** (a and b), **II** (c and d), **IV** (e and f), and **V** (g and h), respectively.

2 nm, respectively. The measurement uncertainty of a single measure is due to the instrument sensitivity: ± 0.5 nm in the height (z axis) and ±2 nm in the x–y plane. The width of the nanotube has been estimated at half-height, and not at the bottom, to reduce the size of errors resulting from effects of tip convolution. In Table 2 are reported the mean, the standard deviation (σ), and the standard error of the mean ($\sigma/\sqrt{N}$) of the maximal height (h) and width at half-height (d) of pristine MWCNT and catalysts **I**–**II** and **IV**–**V**, evaluated by profile analyses of high-resolution AFM images. For each catalyst and for pristine MWCNTs, we have identified 25 dispersed nanotubes, and a statistical analysis has been made on this sample. The MWCNTs and catalysts shown in Figure 7 are well representative of the measured samples.

For comparison in Table 2 are reported the height and width of unmodified MWCNTs.[17a] As we expect, the functionalized MWCNTs are higher and wider than the unmodified nanotubes and show a uniform diameter along the entire length of the MWCNT. This is the proof that the enzyme is adsorbed on the entire tube.

High-resolution AFM images of catalyst **II** are reported in Figure 7d. The surface is smooth, and h and d are 69.0 ± 0.5 and 100 ± 2 nm, respectively (Figure 7f). Catalysts **I** and **II** have comparable heights but different widths: the dimensions of the second system appear reduced to about 60 nm. We can speculate that a stronger interaction between PDDA and a functionalized nanotube could reduce the bond distance and then the size of the catalyst **II**; nevertheless, the low values of the immobilization yields observed in this case (see Table 1, entries 6–11) could also reasonably justify the observed reduced size. The AFM analysis of catalyst **IV** (Figure 7g) showed a remarkable roughness and the presence of nonuniform coating that can be attributed to different bond strengths (i.e., hydrophobic instead of ion exchange interactions) between DERA and pristine carbon nanotubes. In addition, the sample of catalyst **IV** analyzed contained a greater amount of loaded enzyme (Table 1, entry 13) with respect to the other catalysts: thus, the influence due to this, upon the increase of the observed thickness, cannot be ruled out. From the image profile, the maximal h is 80.0 ± 0.5 nm and d is 210 ± 2 nm. Also catalyst **V** (Figure 7j) shows a considerable roughness; again, the presence of PBA reduces the thickness of catalyst **V**, probably due to a more intense interaction with DERA. The maximal h and d values are, respectively, 112.3 ± 0.5 nm and 98 ± 2 nm.

Determination of the Kinetic Parameters. Kinetic parameters were determined for the most active catalyst **I** by measuring the initial rates of the reaction with 2-deoxy-D-ribose-5-phosphate (DRP) in Tris-HCl buffer (100 mM, pH 7.5) at 25 °C. Nine concentrations of DRP (ranging from 0.05 to 2.5 mM) were used to determine the reaction rates. The K_m and V_{max} were calculated by plotting data in both Lineweaver–Burk and nonlinear regression plots. Results are reported in Table 3.

Irrespective of the regression method used, catalyst **I** showed a V_{max} higher than native DERA (and a lower value of K_m), suggesting a better interaction between the enzyme and the substrate following the process of immobilization. These data are in accordance with data previously reported in the literature for the immobilization of DERA on other supports.[10a]

Storage Stability and Reusability Properties. A significant advantage connected to the immobilization of enzymes can derive from their increased stability and the possibility of reuse in successive cycles. In previous studies, DERA showed a good storage stability at 4 °C after microwave-assisted covalent immobilization.[10c] The storage stabilities of DERA and catalyst **I** were then evaluated by measuring the enzyme activity at specific intervals of time (0–15 days) at 25 °C. The catalyst was previously stored at 4 °C in sealed bottles, and at each time point the enzyme activity was measured.

Catalyst **I** retained almost the full activity over the period of time studied, while DERA showed a decrease of activity after the first 5 days, thereby reaching a value of ca. 80% of residual activity after 15 days (Figure 8). These data confirm the optimal behavior in terms of storage stability of catalyst **I**. The reusability properties showed similar trends. In this latter case, the activity of catalyst **I** was determined by recording the time-dependent decrease of the absorbance at 340 nm (NADH consumption) in the previously described activity assay. The catalyst was recovered by centrifugation, washed to remove the substrate, and used again for successive five runs. Under these

dx.doi.org/10.1021/cs500511c | ACS Catal. 2014, 4, 3059–3068

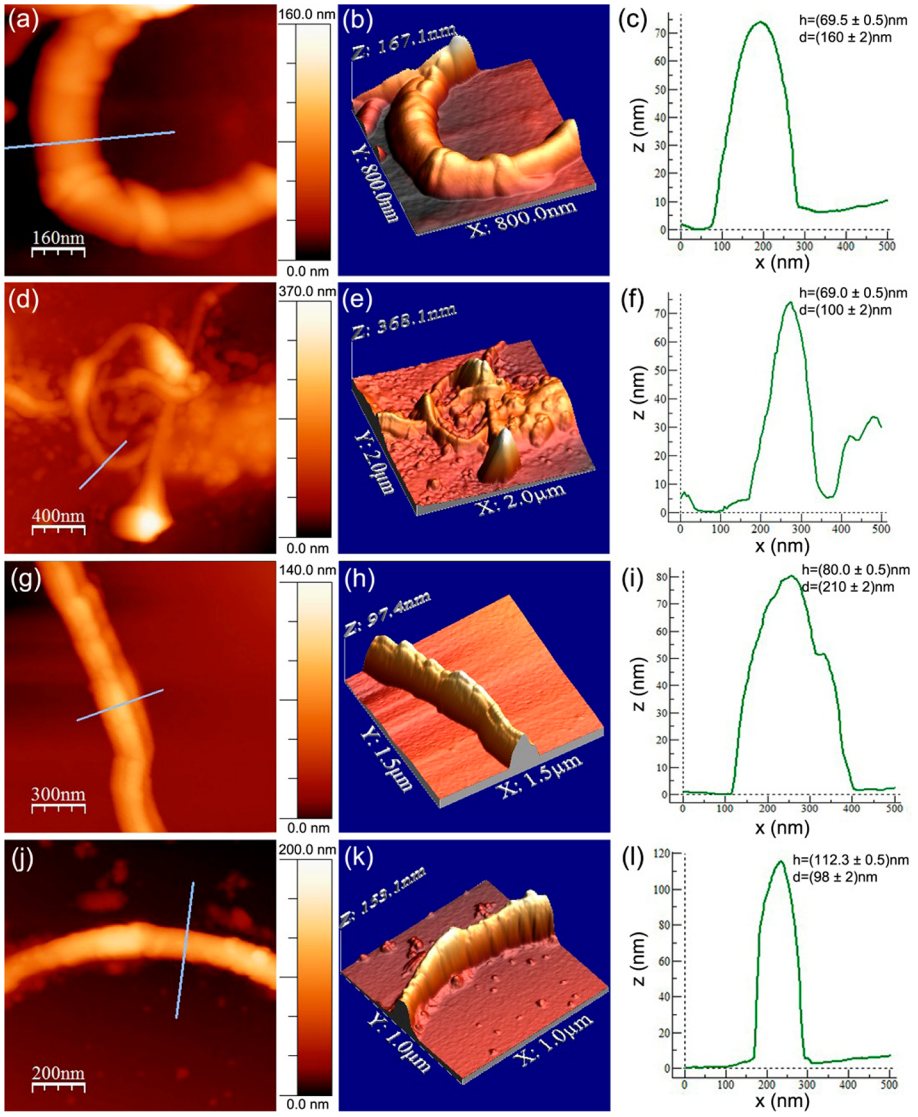

Figure 7. High resolution AFM images (bidimensional, tridimensional, and image profiles) of catalysts **I** (a, b, and c), **II** (d, e, and f), **IV** (g, h, and i), and **V** (j, k, and l), respectively.

Table 2. Mean, Standard Deviation (σ), and Standard Error of Mean ($\sigma/\sqrt{N}$) of the Maximal Height (h) and Width at Half-Height (d) of Pristine MWCNT and Catalysts I–II and IV–V, Evaluated by Profile Analyses of AFM Images[a]

Catalyst[b]	h (nm)	σ_h (nm)	$\sigma_h/\sqrt{N}$ (nm)	d (nm)	σ_d (nm)	$\sigma_d/\sqrt{N}$ (nm)
MWCNT[c]	46	±13	±6	64	±13	±6
I[d]	73	±24	±10	155	±25	±10
II[d]	69	±16	±7	107	±15	±7
IV[d]	73	±14	±6	215	±13	±6
V[d]	121	±20	±9	97	±14	±6

[a]See Figure 7. [b]Catalytic systems: **I** = ox-MWCNTs/DERA; **II** = ox-MWCNTs/PDDA/DERA; **IV** = MWCNTs/DERA; **V** = MWCNTs/PBA/DERA. [c]See ref 17a. [d]For the support/DERA ratio of analyzed catalysts **I**–**II** and **IV**–**V**, see comments in Figure 6.

Table 3. Kinetic Parameters for DERA and Catalyst I[a]

Method	K_m (mM)		V_{max} (ΔAbs/min·μg enz)	
	DERA	catalyst **I**	DERA	catalyst **I**
Lineweaver–Burk	0.55	0.34	0.171	0.198
nonlinear regression	0.64	0.28	0.125	0.297

[a]All experiments were carried out in triplicate using free and immobilized DERA. Average errors in kinetic parameters were 2–4% for K_m and 1–3% for V_{max}.

experimental conditions, catalyst **I** retained up to 85% of the initial activity, confirming its recyclability (see Figure S2 in the Supporting Information).

Acetaldehyde Tolerance. It is well-known from the literature that DERA shows a low tolerance to high aldehyde concentrations.[28] To investigate the tolerance of catalyst **I** toward acetaldehyde,[10b] as a selected substrate, 0.2 U of catalyst was incubated in TEA (50 mM, pH 7.5) containing 300 mM of acetaldehyde (200 μL) at 25 °C for 0–30 min. The samples were recovered by centrifugation and washed with TEA, and the DRP cleavage activity was measured as previously reported. As shown in Figure 9, the activity of DERA decreased to 20% after 30 min, while catalyst **I** retained more than 80% of its activity. The inactivation of DERA by acetaldehyde (or others aldehydes) is mainly due to formation of Schiff bases with lysine residues. It is reasonable to suggest that the observed

dx.doi.org/10.1021/cs500511c | ACS Catal. 2014, 4, 3059–3068

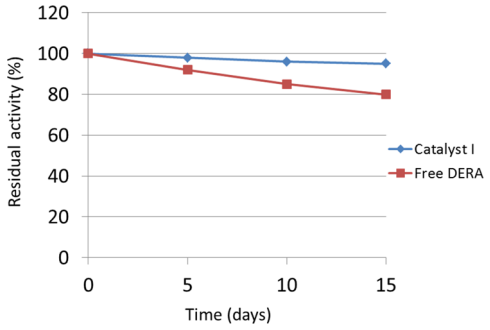

Figure 8. Storage stability of free DERA and catalyst **I**.

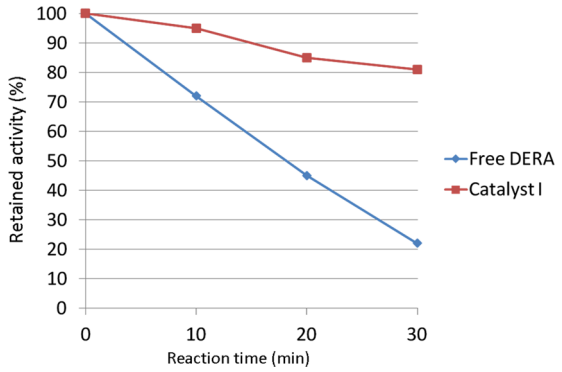

Figure 9. Acetaldehyde tolerance of free DERA and catalyst **I**.

increased tolerance of catalyst **I** can result from the interaction between the positively charged lysines of DERA and negatively charged support (ox-MWCNTs) that could mask in part the nucleophilic centers, making them low reactive toward the excess of aldehyde.[29] On the other hand, factors affecting the "microenvironment engineering", that is the generation of a hydrophilic environment around the enzyme (or just some areas) that will reduce the local aldehyde content, or even just a more rigid conformation of the enzyme that can remain active after modification, cannot be completely ruled out.[29d] Note that the tolerance of catalyst **I** to acetaldehyde was higher than that previously described for DERA when supported on interparticle pore type mesoporous silica (that is ca. 50%, after 30 min).[10b]

Cross-Aldol Condensation. The cross-aldol condensation is a chemical transformation specific for DERA with respect to other aldolases. The versatility of catalyst **I** in this reaction was evaluated analyzing the reactivity of acetaldehyde **1**. In particular, we studied the condensation of **1** alone (self-condensation) or in the presence of chloro-acetaldehyde **2**, as a representative electrophilic acceptor (Scheme 2). Note that only a few examples of this process are reported in the literature.[30] Briefly, catalyst **I** (100 mM) in TEA-HCl buffer (500 μL, pH 7.5) was stirred with **1** (500 mM) alone or in the presence of **2** (500 mM) for 24 h at 25 °C. After workup, the crude was oxidized with $Ca(ClO)_2$ at 5−20 °C (pH 3, adjusted with phosphoric acid) to convert lactol intermediates **A** to stable β−hydroxy-δ-lactones, 4-hydroxy-6-methyltetrahydro-2H-pyran-2-one **3**, and 4-hydroxy-6-chloromethyltetrahydro-2H-pyran-2-one **4**, respectively (Scheme 2).[30] The reactions with native DERA were also performed as references. Under these experimental conditions, the β−hydroxy-δ-lactones **3** and **4** were obtained in 81% and 89% yield, respectively (Scheme 2, Table 4). It is noteworthy that, irrespective of reaction conditions, catalyst **I** was more efficient than DERA, in which case compounds **3** and **4** were only obtained in 46% and 34% yield, respectively (Table 4, entries 1 and 3 versus entries 2 and 4).

Table 4. Cross-Aldol Condensation of Acetaldehyde 1 and Chloroacetaldehyde 2 with Native DERA or Calalyst I

Entry	Aldehyde	Catalyst	Product	Conversion (%)	Yield (%)
1	**1**	DERA	**3**	>98%	46
2	**1**	Catalyst **I**	**3**	>98%	81
3	**1** + **2**	DERA	**4**	>98%	34
4	**1** + **2**	Catalyst **I**	**4**	>98%	89

CONCLUSIONS

The immobilization of DERA on MWCNTs was studied for the first time, and a versatile procedure was established. The efficiency of the immobilized DERA was found to depend on the employed procedure. The absorption of DERA, based on the direct ionic exchange interactions with ox-MWCNTs, afforded the best system (catalyst **I**). The activity of catalyst **I** reached a maximum (1.0 U) at a support/DERA ratio value of 35:1, and it decreased by further increasing the concentration of DERA, probably due to close packing effects.[17] The deposition of PDDA (catalyst **II**), as well as the presence of the PDDA layer between DERA and MWCNTs (catalyst **III**), decreased both the activity and the immobilization yield. Slightly better results were obtained by direct adsorption of DERA on pristine MWCNTs (catalyst **IV**) or by formation of supramolecular aggregations with the PBA/MWCNTs support (catalyst **V**). The morphology of catalysts **I**−**II** and **IV**−**V** was studied by SEM and AFM techniques, which were shown to be powerful tools to monitor the effects that the different procedures used

Scheme 2. Cross-Aldol Condensation of Acetaldehyde 1 and Chloroacetaldehyde 2 with Native DERA or Catalyst I

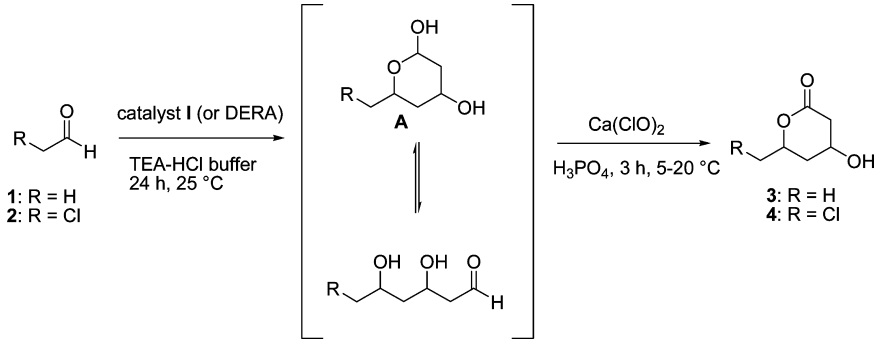

dx.doi.org/10.1021/cs500511c | ACS Catal. 2014, 4, 3059−3068

for the anchoring of DERA may exert on the morphological aspects of the resulting catalysts. From a kinetic point of view, catalyst **I** showed higher V_{max} and lower K_m values than DERA, and it was stable enough to be stored and used for at least five runs. The synthetic utility of catalyst **I** was tested in the cross-aldol condensation of acetaldehyde **1** alone or in the presence of chloroaldehydes **2** as electrophilic acceptor. The β-hydroxy-δ-lactone derivatives **3** and **4** were obtained in 81% and 89% yield, respectively, depending on the reaction conditions, with the best performance being obtained in the cross-aldol reaction of acetaldehydes **1** and **2** with catalyst **I** (89% yield). It is interesting to note that the latter was more efficient than native DERA, suggesting an effective role of the immobilization procedure on the reactivity of the enzyme.

EXPERIMENTAL SECTION

Reagents and Materials. Multiwalled carbon nanotubes (MWCNTs), 2-deoxyribose 5-phosphate aldolase (DERA) recombinant K12 from *E. coli* (EC 4.1.2.4), 2-deoxy-D-ribose-5-phosphate (DRP), pyrenebutyric acid (PBA, pK_a = 4.8), triethanolamine (TEA), triose-phosphate isomerase (TPI), glycerol-3-phosphate dehydrogenase (GDH), ethyl acetate (EtOAc), poly(diallyl dimethylammonium chloride) PDDA, acetaldehyde, and chloroacetaldehyde were purchased from Sigma-Aldrich. All spectrophotometric measurements were made with a Varian Cary50 UV−vis spectrophotometer equipped with a Peltier with a single cell holder. Thin layer chromatography (TLC) was carried out using a Merck platen Kieselgel 60 F254. ^{1}H and ^{13}C NMR spectra were recorded on a Bruker (400 MHz) spectrometer. GC−MS analysis was performed on GC−MS QP5050 Shimadzu apparatus using an SPB column (25 m, 0.25 mm film thickness) and an isothermal temperature profile of 100 °C for 2 min, followed by a 10 °C min^{-1} temperature gradient to 280 °C for 25 min. The injector temperature was 280 °C. Chromatography-grade helium was used as the carrier gas with a flow of 2.7 mL·min^{-1}. Mass spectra were recorded on a Varian instrument with an electron beam of 70 eV. Quantitative analyses were performed by using dodecane as the internal standard. All experiments were done in triplicate using native and immobilized DERA.

Preparation of Catalysts. *Oxidation of MWCNTs.* Multiwalled carbon nanotubes (MWCNTs, >95% purity, inner diameter 5−10 nm and outer diameter 10−30 nm, length 0.5−50 μm) were treated with a concentrated sulfuric acid (98%)/nitric acid (65%) mixture (3:1 v/v) in a sonication bath, for 4 h. The resulting solution was diluted with deionized water and extensively washed by consecutive sonication/centrifugation steps until the pH became neutral. The oxidized nanotubes (ox-MWCNTs) were lyophilized and stored at room temperature as a dry powder.

*Preparation of Catalyst **I**: Ox-MWCNTs/DERA.* Different amounts of DERA (ranging from 0.1 to 0.02 mg) were adsorbed on ox-MWCNTs (1.0 mg) in sodium acetate buffer (0.1 M, pH 5.5) under orbital shaking at room temperature (40 min at 150 rpm). The excess enzyme was removed by centrifugation, and the surnatant was used for immobilization and activity yield calculations. The catalyst was washed several times with buffer in order to ensure the complete removal of unbounded enzyme. The absence of DERA in the washing waters was confirmed by the activity assay and the Bradford method.

*Preparation of Catalyst **II**: Ox-MWCNTs/PDDA/DERA.* Ox-MWCNTs (0.5 mg) were dispersed in 1.0 mL of 0.5 M NaCl solution containing 1.0 mg of PDDA by combination of sonication (5 min, rt) and orbital shaking (20 min, rt, 170 rpm). The excess PDDA was removed by centrifugation at 6000 rpm × 20 min. An additional washing cycle was necessary to remove the PDDA residue (6000 rpm × 20 min). Then, PDDA wrapped carbon nanotubes were dispersed in 0.5 mL of 0.1 M sodium acetate buffer solution (pH 5.5) containing DERA (ranging from 0.05 to 0.014 mg) and shaken (40 min, rt, 150 rpm). The excess enzyme was removed by centrifugation at 6000 rpm for 20 min (an additional washing cycle was necessary).

*Preparation of Catalyst **III**: Ox-MWCNTs/DERA/PDDA.* Ox-MWCNTs/DERA (0.5 mg) were dispersed in 1.0 mL of 0.5 M NaCl solution (pH 7.0) containing 1.0 mg of PDDA by combination of sonication (5 min, rt) and orbital shaking (20 min, rt, 170 rpm). The excess PDDA was removed by centrifugation at 6000 rpm for 20 min. An additional washing cycle was necessary to remove the PDDA residue (6000 rpm × 20 min).

*Preparation of Catalyst **IV**: MWCNTs/DERA.* MWCNTs (0.5 mg) were dispersed in 0.4 mL of 0.1 M sodium acetate buffer (pH 5.5) by prolonged sonication (30 min). A DERA solution in the same buffer (0.1 mL containing DERA ranging from 0.05 to 0.011 mg) was then added and shaken (40 min, rt, 150 rpm). The excess enzyme was removed by centrifugation at 6000 rpm for 20 min. An additional washing cycle was necessary to remove the enzyme residue.

*Preparation of Catalyst **V**: MWCNTs/PBA/DERA.* MWCNTs (4 mg) were dispersed in 20 mL of EtOH containing 40 mg of PBA by combination of sonication (2 h) and shaking (150 rpm overnight). MWCNTs/PBA (0.5 mg) were centrifuged at 6000 rpm and the water removed. After centrifugation, the black solid was dispersed in 0.1 M Na acetate buffer solution (0.5 mL, pH 5.5) containing various amount of DERA (ranging from 0.05 to 0.014 mg) and shaken (40 min, rt, 150 rpm). The excess enzyme was removed by centrifugation at 6000 rpm for 20 min. An additional washing cycle was necessary to remove the enzyme residue.

Determination of Activity, Activity Yield and Immobilization Yield. The activity of native and immobilized enzyme was measured by following the oxidation of NADH in a coupled assay converting glyceraldehyde 3-phosphate, one of the DRP cleavage products, to glycerol 3-phosphate by TPI and GDH (Scheme 1). The reaction mixture (1.5 mL) contained 100 mM Tris-HCl buffer (pH 7.5), 0.1 mM NADH, 1 mM DRP, 3 μL of TPI/GDH (according to the protocol described in ref 10b), and 2.8 μg of native or immobilized DERA. The assay started after the addition of the enzyme, and the consumption of NADH was monitored at 340 nm. The extinction coefficient of NADH was taken to be 6.22 mM^{-1} cm^{-1}. The activity was defined as the amount of DERA required to catalyze the cleavage of 1 μmol of DRP per minute at pH 7.5 and 25 °C. The activity of immobilized DERA was expressed as activity unit per milligram of support and as activity and immobilization yield. Spectrophotometric data were analyzed with Cary WinUV software. All experiments were carried out in triplicate using free and immobilized DERA.

SEM and AFM Characterization of Catalysts. The surface morphology of the samples has been studied by scanning electron microscopy (SEM) analysis, making use of a Zeiss, LEO 1530 apparatus equipped with a field emission electron gun, while atomic force microscopy (AFM) was performed with a Digital Dimension D5000 instrument with a

dx.doi.org/10.1021/cs500511c | ACS Catal. 2014, 4, 3059−3068

Nanoscope IV controller, using commercial silicon tips (frequency range 51−94 kHz) scanned by means of a Veeco Nanoman closed loop XY head. For the SEM and AFM analysis, different solutions of the samples were prepared. In particular, the samples were dispersed in Milli-Q water, in order to prevent the enzyme denaturation. All the solutions were sonicated for 5 min at room temperature, and a drop of each solution was taken and deposited onto silicon substrates (Si). At the end, the obtained samples deposited on Si were subjected to annealing at 50 °C to quickly evaporate the solvent (water). First SEM analysis was done to identify individual dispersed nanotubes, and then, through a mapping of Si substrate, same nanotubes were detected with AFM. At first SEM analysis was done to identify individual dispersed nanotubes, namely 25 nanotubes for each sample, and then, through a mapping of Si substrate, the same nanotubes were detected with AFM. The mean value, the standard deviation, and the standard error of the mean of the maximal height and width at half-height were obtained by a statistical analysis of profiles of high-resolution AFM images.

Determination of the Kinetic Constants. The kinetic constants of native and immobilized DERA were determined by measuring the initial rates of the reaction with DRP as the substrate in Tris-HCl buffer (100 mM, pH 7.5) at 25 °C. Nine concentrations of DRP, ranging from 0.05 to 2.5 mM, were used to determine the reaction rates. The K_m and V_{max} were calculated by plotting data in Lineweaver−Burk and nonlinear regression plots.

Storage Stability. The storage stability of native and immobilized DERA was estimated by measuring enzyme activity for specific time intervals (0−15 days) at 25 °C. The catalyst was stored at 4 °C in sealed bottles, and at each time point, an appropriate amount was taken, and the enzyme activity was measured as described above.

Enzyme Recycling. The activity of catalyst **I** was determined by recording the time-dependent decrease in absorbance at 430 nm (NADH consumption) in the described coupled assay. The catalyst was then recovered by centrifugation (6000 rpm for 20 min), washed to remove the substrate, and reused again for the cleavage of fresh DRP.

Acetaldehyde Tolerance of Native and Immobilized DERA. To investigate the tolerance of DERA to a high concentration of aldehyde, 0.5 mg of catalyst **I** was incubated in a 100 mM TEA solution (pH 7.5), containing 300 mM acetaldehyde **1** (500 μL) at 25 °C. After 20 min an aliquot was removed (100 μL), catalyst **I** was recovered by centrifugation, and the DRP cleavage activity was measured. The experiments were performed in triplicate.

Cross-Aldol Condensations. Catalyst **I** (0.1 U) in TEA-HCl buffer (500 μL, pH 7.5) was treated with acetaldehyde **1** (500 mM) alone or in the presence of chloroacetaldehyde **2** (500 mM) for 24 h at 25 °C. As a general workup procedure, the pH of the reaction was lowered to 4.5 using phosphoric acid (in the case of heterogeneous conditions, the catalyst **I** was removed from the reaction mixture by centrifugation). A small amount of Na_2SO_4 was added in order to facilitate the extraction of reaction products with EtOAc (3 × 5.0 mL). The collected organic extracts were cooled to 0 °C, the pH was adjusted to 3 with phosphoric acid, and a small excess of $Ca(ClO)_2$ was added, keeping the pH between 2 and 6 (with phosphoric acid) and the temperature in the range between 5 and 20 °C. After 3.0 h, chlorine was driven out by bubbling nitrogen and EtOAc was evaporated under vacuum. The yellow oil residue was purified by analytical TLC (Silica gel 60 F254-Merk, running solvent 1-butanol, acetic acid, and H_2O, using *p*-anisaldehyde as developing solution) to yield δ-lactones 4-hydroxy-6-methyltetrahydro-2H-pyran-2-one **3** or 4-hydroxy-6-chloromethyltetrahydro-2H-pyran-2-one **4**, in quantitative conversion and 81% and 89% yield, respectively.

4-Hydroxy-6-methyltetrahydro-2H-pyran-2-one ***3***. Oil; ^{1}H NMR (400 MHz, acetone-d_6) δ ppm: 4.76 (1H, m), 4.10−4.40 (m, 2H), 2.40−2.50 (1H, m), 1.94 (1H, m), 1.71 (1H, m), 1.29 (3H, m, CH_3); ^{13}C NMR (125 MHz, acetone-d_6) δ ppm: 170.6, 72.7, 63.1, 39.1, 38.2, 21.8; GC-MS: 131 $(M + H)^+$.

4-Hydroxy-6-chloromethyltetrahydro-2H-pyran-2-one ***4***. Oil; ^{1}H NMR (400 MHz, acetone-d_6) δ ppm: 4.50 (1H, m), 3.75−3.58 (3H, m), 2.40−2.70 (2H, m), 1.80−2.30 (2H, m); ^{13}C NMR (125 MHz, acetone-d_6) δ ppm: 169.3, 74.2, 65.4, 48.5, 40.0, 37.1; GC-MS: 165 $(M + H)^+$.

■ ASSOCIATED CONTENT

Supporting Information

Steps for identification of functionalized carbon nanotubes: Figure S1 to explain the approach followed for the selection of the sample portion during SEM and AFM analyses of catalyst **II**; Figure S2 describing the results of the reusability study on catalyst **I**. This material is available free of charge via the Internet at http://pubs.acs.org.

■ AUTHOR INFORMATION

Corresponding Authors

*(M.C.) E-mail: marcello.crucianelli@univaq.it; fax: (+39) 0862-433753.

*(R.S.) E-mail: saladino@unitus.it; fax: (+39) 0761-357242.

Notes

The authors declare no competing financial interest.

[‖](F.S.) Current e-mail address: f.subrizi@ucl.ac.uk.

■ ACKNOWLEDGMENTS

F.S. thanks University of L'Aquila for a research grant. M.C. thanks "Fondazione Cassa di Risparmio della Provincia dell'Aquila" for a research contribution.

■ REFERENCES

(1) (a) Samland, A. K.; Sprenger, G. A. *Appl. Microbiol. Biotechnol.* **2006**, *71*, 253−264. (b) Mestres, R. *Green Chem.* **2004**, *6*, 583−603.

(2) Clapés, P.; Fessner, W. D.; Sprenger, G. A.; Samland, A. K. *Curr. Opin. Chem. Biol.* **2010**, *14*, 154−167.

(3) (a) Han, T. K.; Zhu, Z.; Dao, M. L. *Curr. Microbiol.* **2004**, *48*, 230−236. (b) Chen, L.; Dumas, D. P.; Wong, C.-H. *J. Am. Chem. Soc.* **1992**, *114*, 741−748. (c) Barbas, C. F.; Wang, Y.-F.; Wong, C.-H. *J. Am. Chem. Soc.* **1990**, *112*, 2013−2014. (d) Valentin-Hansen, P.; Boetius, F.; Hammer-Jespersen, K.; Svendsen, I. *Eur. J. Biochem.* **1982**, *125*, 561−566.

(4) (a) Gijsen, H. J. M.; Qiao, L.; Fitz, W.; Wong, C.-H. *Chem. Rev.* **1996**, *96*, 443−474. (b) Gijsen, H. J. M.; Wong, C.-H. *J. Am. Chem. Soc.* **1995**, *117*, 7585−7591. (c) Gijsen, H. J. M.; Wong, C.-H. *J. Am. Chem. Soc.* **1994**, *116*, 8422−8423.

(5) (a) Bolt, A.; Berry, A.; Nelson, A. *Arch. Biochem. Biophys.* **2008**, *474*, 318−330. (b) Dean, S. M.; Greenberg, W. A.; Wong, C.-H. *Adv. Synth. Catal.* **2007**, *349*, 1308−1320. (c) Whalen, L. J.; Wong, C.-H. *Aldrichim. Acta* **2006**, *39*, 63−71.

(6) Liu, J.; Wong, C.-H. *Angew. Chem., Int. Ed.* **2002**, *41*, 1404−1407.

(7) Liu, J.; Hsu, C.-C.; Wong, C.-H. *Tetrahedron Lett.* **2004**, *45*, 2439−2441.

(8) (a) Ikunaka, M. *Org. Process Res. Dev.* **2007**, *11*, 495−502. (b) Panke, S.; Wubbolts, M. *Curr. Opin. Chem. Biol.* **2005**, *9*, 188−194.

(c) De Santis, G.; Liu, J. J.; Clark, D. P.; Heine, A.; Wilson, I. A.; Wong, C. H. *Bioorg. Med. Chem.* **2003**, *11*, 43−52. (d) Bertau, M. *Curr. Org. Chem.* **2002**, *6*, 987−1014.
(9) (a) Yin, X.; Wang, Q.; Zhao, S.-J.; Du, P.-F.; Xie, K.-L.; Jin, P.; Xie, T. *African J. Biotechnol.* **2011**, *10*, 16260−16266. (b) Fernandez-Lafuente, R. *Enzyme Microb. Technol.* **2009**, *45*, 405−418. (c) Sakuraba, H.; Yoneda, K.; Yoshihara, K.; Satoh, K.; Kawakami, R.; Uto, R.; Tsuge, H.; Takahashi, K.; Hori, H.; Ohshima, T. *Appl. Environ. Microbiol.* **2007**, *73*, 7427−7434. (d) Greenberg, W. A.; Varvak, A.; Hanson, S. R.; Wong, K.; Huang, H.; Chen, P.; Burk, M. J. *Proc. Natl. Acad. Sci. U.S.A.* **2004**, *101*, 5788−5793. (e) Wong, C.-H.; Garcia-Junceda, E.; Chen, L.; Blanco, O.; Gijsen, H. J. M.; Steensma, D. H. *J. Am. Chem. Soc.* **1995**, *117*, 3333−3339.
(10) (a) Wang, A.; Gao, W.; Zhang, F.; Chen, F.; Du, F.; Yin, X. *Bioprocess Biosyst. Eng.* **2012**, *35*, 857−863. (b) Nara, T. Y.; Togashi, H.; Ono, S.; Egami, M.; Sekikawa, C.; Suzuki, Y.-h.; Masuda, I.; Ogawa, J.; Horinouchi, N.; Shimizu, S.; Mizukami, F.; Tsunoda, T. *J. Mol. Catal. B* **2011**, *68*, 181−186. (c) Wang, A.; Wang, M.; Wang, Q.; Chen, F.; Zhang, F.; Li, H. *Bioresour. Technol.* **2011**, *102*, 469−474.
(11) For recent reviews on this general topic, see: (a) Brena, B.; González-Pombo, P.; Batista-Viera, F. *Methods Mol. Biol.* **2013**, *1051*, 15−31. (b) Barbosa, O.; Torres, R.; Ortiz, C.; Berenguer-Murcia, A.; Rodrigues, R. C.; Fernandez-Lafuente, R. *Biomacromolecules* **2013**, *14*, 2433−2462. (c) Rodrigues, R. C.; Ortiz, C.; Berenguer-Murcia, A.; Torres, R.; Fernández-Lafuente, R. *Chem. Soc. Rev.* **2013**, *42*, 6290−6307. (d) Zhou, Z.; Hartmann, M. *Chem. Soc. Rev.* **2013**, *42*, 3894−3912. (e) Verma, M. L.; Barrow, C. J.; Puri, M. *Appl. Microbiol. Biot.* **2013**, *97*, 23−39. (f) Hwang, E. T.; Gu, M. B. *Eng. Life Sci.* **2013**, *13*, 49−61. (g) Rajkumar, K.; Palla, S.; Paladugu, A.; Reddy, E. R.; Reddy, K. R. *Int. Res. J. Pharm.* **2013**, *4*, 36−44. (h) Tran, D. N.; Balkus, K. J., Jr. *ACS Catal.* **2011**, *1*, 956−968. (i) Garcia-Galan, C.; Berenguer-Murcia, A.; Fernandez-Lafuente, R.; Rodrigues, R. C. *Adv. Synth. Catal.* **2011**, *353*, 2885−2904.
(12) Cao, L.; Schmid, R. D. *Carrier-Bound Immobilized Enzymes: Principles, Application and Design*; Wiley-VCH Verlag GmbH & Co.: Weinheim, 2006.
(13) Feng, W.; Ji, P. *Biotechnol. Adv.* **2011**, *29*, 889−895.
(14) Tasis, D.; Tagmatarchis, N.; Bianco, A.; Prato, M. *Chem. Rev.* **2006**, *106*, 1105.
(15) Hanefeld, U.; Gardossi, L.; Magner, E. *Chem. Soc. Rev.* **2009**, *38*, 453−468.
(16) Asuri, P.; Karajanagi, S. S.; Sellitto, E.; Kim, D.-Y.; Kane, R. S.; Dordick, J. S. *Biotechnol. Bioeng.* **2006**, *95*, 804−811.
(17) (a) Subrizi, F.; Crucianelli, M.; Grossi, V.; Passacantando, M.; Pesci, L.; Saladino, R. *ACS Catal.* **2014**, *4* (3), 810−822. (b) Bussamara, R.; Dall'Agnol, L.; Schrank, A.; Fernandes, K. F.; Vainstein, M. H. *Enzyme Res.* **2012**, Article ID 329178 (http://dx.doi.org/10.1155/2012/329178). (c) Lei, C.; Shin, Y.; Liu, J.; Ackerman, E. J. *J. Am. Chem. Soc.* **2002**, *124*, 11242−11243.
(18) Yiu, H. H. P.; Wright, P. A. *J. Mater. Chem.* **2005**, *15*, 3690−3700.
(19) (a) Decher, G. *Science* **1997**, *277*, 1232−1237. (b) Decher, G.; Schmitt, J. *Prog. Colloid Polym. Sci.* **1992**, *89*, 160−164.
(20) (a) Mateo, C.; Fernandes, B.; Van Rantwijk, F.; Stolz, A.; Sheldon, R. A. *J. Mol. Catal. B* **2006**, *38*, 154−157. (b) Wilson, L.; Illanes, A.; Abián, O.; Pessela, B. C. C.; Fernández-Lafuente, R.; Guisán, J. M. *Biomacromolecules* **2004**, *5*, 852−857. (c) Abián, O.; Wilson, L.; Mateo, C.; Fernández-Lorente, G.; Palomo, J. M.; Fernández-Lafuente, R.; Guisán, J. M.; Re, D.; Tam, A.; Daminatti, M. *J. Mol. Catal. B* **2002**, *19*−*20*, 295−303. (d) Abián, O.; Mateo, C.; Fernández-Lorente, G.; Palomo, J. M.; Fernández-Lafuente, R.; Guisán, J. M. *Biocatal. Biotransfor.* **2001**, *19*, 489−503.
(21) (a) Iamsamai, C.; Soottitantawat, A.; Ruktanonchai, U.; Hannongbua, S.; Dubas, S. T. *Carbon* **2011**, *49*, 2039−2045. (b) Lee, J.; Park, S.-J.; Moon, Y.-K.; Kim, S.-H.; Koh, K. *Korean J. Chem. Eng.* **2009**, *26*, 1790−1794.
(22) Ziółkowska, D.; Shyichuk, A.; Zelazko, K. *Polimery* **2012**, *57*, 303−305.
(23) (a) Gupta, N.; Rathi, P.; Singh, R.; Goswami, V. K.; Gupta, R. *Appl. Microbiol. Biotechnol.* **2005**, *67*, 648−653. (b) Heinsman, N. W. J. T.; Schroën, C. G. P. H.; Van der Padt, A.; Franssen, M. C. R.; Boom, R. M.; Van't Riet, K. *Tetrahedron: Asymmetry* **2003**, *14*, 2699−2704. (c) Kirk, O.; Christensen, M. W. *Org. Process Res. Dev.* **2002**, *6*, 446−451.
(24) Larson, T. A.; Olson, A. J.; Goodsell, D. S. *Chem. Biol.* **1998**, *6*, 421.
(25) (a) Das, D.; Das, P. K. *Langmuir* **2009**, *25*, 4421−4428. (b) Karajanagi, S. S.; Vertegel, A. A.; Kane, R. S.; Dordick, J. S. *Langmuir* **2004**, *20*, 11594−11599.
(26) For some examples of this procedure, see: (a) Parimi, N. S.; Umasankar, Y.; Atanassov, P.; Ramasamy, R. P. *ACS Catal.* **2012**, *2*, 38−44. (b) Lerner, M. B.; Resczenski, J. M.; Amin, A.; Johnson, R. R.; Goldsmith, J. I.; Johnson, A. T. C. *J. Am. Chem. Soc.* **2012**, *134*, 14318−14321. (c) Karachevtsev, V. A.; Stepanian, S. G.; Glamazda, A. Y.; Karachevtsev, M. V.; Eremenko, V. V.; Lytvyn, O. S.; Adamowicz, L. *J. Phys. Chem. C* **2011**, *115*, 21072−21082. (d) Jönsson-Nieddziolka, M.; Kaminska, A.; Opallo, M. *Electrochim. Acta* **2010**, *55*, 8744−8750. (e) Pang, H. L.; Liu, J.; Hu, D.; Zhang, X. H.; Chen, J. H. *Electrochim. Acta* **2010**, *55*, 6611−6616.
(27) Horcas, I.; Fernandez, R.; Gomez-Rodrìguez, J. M.; Colchero, J.; Gomez-Herrero, J.; Baro, A. M. *Rev. Sci. Instrum.* **2007**, *78*, 013705/1−013705/8.
(28) Stefan, J.; Martin, S. M.; Michael, W.; Iris, H.; Ruud, L.; Marcel, W.; Daniel, M. *Biotechnol. J.* **2006**, *1*, 537−548.
(29) (a) Moelans, D.; Cool, P.; Baeyens, J.; Vansant, E. F. *Catal. Commun.* **2005**, *6*, 307−311. (b) Matsumura, I.; Wallingford, J. B.; Surana, N. K.; Vize, P. D.; Ellington, A. D. *Nat. Biotechnol.* **1999**, *17*, 696−701. (c) Habeeb, A. F. S. A.; Hiramoto, R. *Arch. Biochem. Biophys.* **1968**, *126*, 16−26. (d) Cao, L. *Curr. Opin. Chem. Biol.* **2005**, *9*, 217−226.
(30) Ošlaj, M.; Cluzeau, J.; Orkić, D.; Kopitar, G.; Mrak, P.; Časar, Z. *PLoS One* **2013**, *8*, e62250.